Vientos—A New Satellite Mission Concept for 3D Wind Measurements by Combining Passive Water Vapor Sounders with Doppler Wind Lidar

Xubin Zeng, Hui Su, Svetla Hristova-Veleva, Derek J. Posselt, Robert Atlas,
Shannon T. Brown, Ross D. Dixon, Eric Fetzer, Thomas J. Galarneau Jr., Michael Hardesty,
Jonathan H. Jiang, Pekka P. Kangaslahti, Amir Ouyed, Thomas S. Pagano,
Oliver Reitebuch, Remy Roca, Ad Stoffelen, Sara Tucker, Anna Wilson,
Longtao Wu, and Igor Yanovsky

KEYWORDS:
Dynamics;
Wind shear;
Wind;
Convective storms;
Satellite
observations;
Machine learning

ABSTRACT: It is challenging to accurately characterize the three-dimensional distribution of horizontal wind vectors (known as 3D winds). Feature-matching satellite cloud top or water vapor fields have been used for decades to retrieve atmospheric motion vectors, but this approach is mostly limited to a single and uncertain pressure level at a given time. Satellite wind lidar measurements are expected to provide more accurate data and capture the line-of-sight wind for clear skies, within cirrus clouds, and above thick clouds, but only along a curtain parallel to the satellite track. Here we propose Vientos—a new satellite mission concept that combines two or more passive water vapor sounders with Doppler wind lidar to measure 3D winds. The need for 3D wind observations is highlighted by inconsistencies in reanalysis estimates, particularly under precipitating conditions. Recent studies have shown that 3D winds can be retrieved using water vapor observations from two polar-orbiting satellites separated by 50 min, with the help of advanced optical flow algorithms. These winds can be improved through the incorporation of a small number of collocated higher-accuracy measurements via machine learning. The Vientos concept would enable simultaneous measurements of 3D winds, temperature, and humidity, and is expected to have a significant impact on scientific research, weather prediction, and other applications. For example, it can help better understand and predict the preconditions for organized convection. This article summarizes recent results, presents the Vientos mission architecture, and discusses implementation scenarios for a 3D wind mission under current budget constraints.

AFFILIATIONS: Zeng and Ouyed—Department of Hydrology and Atmospheric Sciences, The University of Arizona, Tucson, Arizona; Su—Department of Civil and Environmental Engineering, Hong Kong University of Science and Technology, Hong Kong, China; Hristova-Veleva, Posselt, Brown, Fetzer, Jiang, Kangaslahti, Pagano, Wu, and Yanovsky—Jet Propulsion Laboratory, California Institute of Technology, Pasadena, California; Atlas*—NOAA/Atlantic Oceanographic and Meteorological Laboratory, Miami, Florida; Dixon—Department of Earth and Atmospheric Sciences, University of Nebraska–Lincoln, Lincoln, Nebraska; Galarneau—NOAA/OAR/National Severe Storms Laboratory, Norman, Oklahoma; Hardesty—Cooperative Institute for Research in Environmental Sciences, University of Colorado Boulder, Boulder, Colorado; Reitebuch—Institut für Physik der Atmosphäre, Deutsches Zentrum für Luft- und Raumfahrt, Oberpfaffenhofen, Germany; Roca—Laboratoire d'Etudes en Géophysique et Océanographie Spatiales (Université de Toulouse III, CNRS, CNES, IRD), Toulouse, France; Stoffelen—Royal Netherlands Meteorological Institute (KNMI), De Bilt, Netherlands; Tucker—Ball Aerospace, Boulder, Colorado; Wilson—Center for Western Weather and Water Extremes, Scripps Institution of Oceanography, University of California, San Diego, La Jolla, California

* Retired

The three-dimensional (3D) distribution of horizontal atmospheric wind vectors (referred to as 3D winds) is an integral part of the Earth system. Dynamic meteorology, a core course for college students in atmospheric science and meteorology, starts by deriving the governing equations for winds based on Newton's law. The ceaseless winds over mid- and high latitudes are driven primarily by the horizontal pressure differences which are, in turn, affected by physical processes in the atmosphere, such as those associated with radiation, turbulence, convection, clouds, and precipitation. Three-dimensional winds interact with clouds, convection, and precipitation. They transport heat, moisture, momentum, aerosols, and trace gases. They also drive ocean circulations and affect sensible and latent heat fluxes between the atmosphere and the underlying land or ocean surfaces. As 3D winds are an important part of Earth system dynamics, their accurate observation is critical for a variety of applications, such as weather and climate forecasting, aerosol and pollution transport, disaster weather monitoring, wind energy generation, aircraft flight planning, and wildfire and volcanic plume movement.

While most variables needed to characterize the state of the atmosphere, such as temperature, humidity, clouds, precipitation, and aerosols, can be measured from space, 3D wind measurements remain a challenge. New missions planned for the coming decade will provide spaceborne estimates of vertical motions in clouds for the very first time using Doppler radar in the European Space Agency (ESA) EarthCARE mission (https://earth.esa.int/eogateway/missions/earthcare) and the NASA Atmosphere Observing System mission (https://aos.gsfc.nasa.gov/). The NASA Investigation of Convective Updrafts (INCUS) mission will estimate convective vertical mass flux from time-differenced radar measurements (https://incus.colostate.edu/). However, none of these planned missions will provide horizontal wind vector estimates.

Conventional observations of horizontal winds, such as from rawinsondes, wind profilers, and airborne dropsondes, have sparse coverage in both space and time, especially over oceans. An international virtual constellation of wind scatterometers provide accurate vector winds, but near the ocean surface only (Stoffelen et al. 2019). Atmospheric motion vectors (AMVs) have been retrieved for decades to represent horizontal winds by feature-matching satellite cloud

top or water vapor fields. But they are available mostly at a single pressure level (for cloud top) or a thick layer (for water vapor) at a given time and location, with relatively large errors due to vertical height assignment and retrieval uncertainties. A spaceborne Doppler wind lidar is expected to provide more accurate wind measurements for clear sky, within optically thin cirrus clouds, and above water clouds (Stoffelen et al. 2020; Baker et al. 2014) along a narrow curtain that is parallel to the satellite track. This was realized for the first time through the ESA's *Aeolus* satellite mission (Reitebuch 2012) for a single line-of-sight wind component only (close to the east–west direction) of horizontal winds, though with great impact (Rennie et al. 2021), suggesting the importance of providing more complete 3D winds. The *Aeolus* mission also demonstrated that Doppler lidar technology can be effectively deployed and operated in the space environment to produce unique and useful wind and aerosol observations.

Because of the importance of 3D winds and the challenges associated with their measurement, improving 3D wind measurements has long been a top priority in the scientific community and government agencies (e.g., NASA, NOAA, ESA) related to weather, climate, and hydrometeorology (e.g., Zeng et al. 2016). For instance, the 2017–2027 Decadal Survey for Earth Science and Applications from Space (National Academies of Sciences, Engineering, and Medicine 2018) recommended 3D winds as one of the seven observables for the Earth System Explorer satellite mission competition, suggesting active and passive methods for obtaining the wind measurements. In response, here we present Vientos[1]—a new satellite mission concept for 3D wind measurements that combines observations from passive water vapor sounders and a Doppler wind lidar. To increase the readability of this paper to readers with diverse backgrounds, we cite the most relevant references only, while a more comprehensive review of prior work can be found in the cited references.

[1] Vientos means "winds" in Spanish; it also stands for Vector winds In Earth Environments Observing System.

Compelling need for 3D wind measurements

As mentioned above, existing observing systems do not provide full global 3D winds. In their absence, reanalysis datasets provide a spatially coherent and temporally continuous representation of the atmospheric state (including 3D winds) by combining output from a weather forecast model with surface-based, aircraft, and satellite observations (including AMVs) in a data assimilation system. In many cases, reanalysis is regarded as equivalent to observations and has been widely used in weather and climate studies. Nevertheless, reanalyses have rather large systematic dynamical errors (Belmonte-Rivas and Stoffelen 2019), and some of these biases can be explored by comparing winds from different reanalysis products.

We recently compared three reanalysis datasets: ERA5 from the European Centre for Medium-Range Weather Forecasts (ECMWF), MERRA-2 from NASA, and CFSv2 from NOAA (Wu et al. 2024). Comparisons were made at 6-hourly intervals on a 0.5° latitude × 0.625° longitude grid from 2017 to 2021 between 60°S and 60°N. When convection occurs with precipitation rate > 0.1 mm h^{-1}, the wind vector differences (WVDs) between reanalyses are greater than 5 m s^{-1} for 30%–50% of the time over many regions, such as the eastern Pacific, Indian Ocean, Atlantic, and some mountain areas at different pressure levels (with the 500 hPa results shown in Fig. S1 in the online supplemental material; https://doi.org/10.1175/BAMS-D-22-0283.2). In contrast, when all conditions are considered, WVDs are much smaller—they are greater than 5 m s^{-1} for about 7%, 6%, and 18% of the data at 700, 500, and 300 hPa, respectively. The mean WVDs are generally larger over ocean than over land because reanalysis products are better constrained by conventional observations over land. Reanalysis datasets differ at the 95% significance level in most regions over the tropics, while the differences are not significant in most regions over the extratropics. This is due to the deviation of winds from the geostrophic balance constraint over the tropics, where multiscale convective

processes play a dominant role (e.g., Stoffelen et al. 2020). This issue is further compounded by the lack of conventional wind observations over most of the tropics.

The above WVDs do not represent the differences in the spatial variability of winds. The horizontal variability of winds can be characterized by two dynamic quantities (vorticity and divergence). These quantities are useful in diagnosing the processes that drive the evolution of convective systems. Large discrepancies in the mean absolute difference in these quantities exist among the three reanalysis datasets, with the difference magnitude comparable to the mean divergence or vorticity (while WVDs are much smaller than mean wind speed) (Wu et al. 2024). Furthermore, the uncertainties in both divergence and vorticity are driven by the horizontal variations of winds, with weak correlations with the WVDs. In contrast, the uncertainty in the vertical variation of winds (i.e., wind shear) is correlated with WVDs (Wu et al. 2024).

These large uncertainties in the reanalysis winds and wind-derived dynamic quantities materialize when exploring trends in extreme precipitation for which intercomparison reveals the lack of robustness of the reanalysis compared to other precipitation datasets (Alexander et al. 2020). They underscore the need for new satellite missions for 3D winds, as emphasized by the 2017–2027 Decadal Survey (National Academies of Sciences, Engineering, and Medicine 2018).

Scientific feasibility of the Vientos concept

The Vientos concept would provide retrievals of 3D AMVs by tracking the movement of water vapor, followed by a bias correction using the more accurate, but very limited in space, wind lidar measurements. Prior studies have also demonstrated that lidar-derived height assignments, along with representing AMVs as winds over a vertical layer, can improve cloud-top AMV retrievals and AMV impacts (Folger and Weissmann 2016). Numerous studies have been published on the feasibility of the feature-matched 3D AMVs, usually using observing system simulation experiments (OSSEs; Zeng et al. 2020). For instance, McCarty et al. (2021) used OSSEs to investigate AMVs and radiances from a constellation of infrared sounders. Posselt et al. (2019) quantitatively assessed the dependence of AMV uncertainties on time interval, AMV matching window size, water vapor content, horizontal gradient, and wind structure. Ouyed et al. (2021) and Apke et al. (2022) showed superior performance of a retrieval technique at the pixel level based on a variational method (i.e., the optical flow method) as compared with a traditional feature-matching method.

Santek et al. (2019a) derived 3D AMVs from Atmospheric Infrared Sounder (AIRS) water vapor measurements over the polar region, taking advantage of *Aqua* satellite's track convergence that provides frequent observations there. Hautecoeur et al. (2020) presented some preliminary efforts to derive 3D winds from Infrared Atmospheric Sounding Interferometer (IASI) water vapor measurements poleward of 45° using the swath overlap of *MetOp-A* and *MetOp-B* satellites, again providing water vapor measurements with small time difference.

More recently, Ouyed et al. (2023) demonstrated the feasibility of retrieving 3D AMVs from 60°N to 60°S using time-differenced water vapor observations from the hyperspectral Cross-track Infrared Sounder (CrIS) and Advanced Technology Microwave Sounder (ATMS) aboard two operational polar-orbiting satellites (*NOAA-20* and *Suomi NPP*). These two satellites have overlapped tracks separated by 50 min. The width of the overlapped swath is ~900 km, with collocated water vapor data in 1° × 1° grids. The grid-level retrieval is enabled by the use of an optical flow method which outperforms the traditional feature-matching method by not requiring a feature to leave grids in order for its movement to be detected. The retrieval does not need a first guess of 3D winds (e.g., using reanalysis data); however, for a gross

error check, the retrieved AMV is flagged if its wind vector difference from the ERA5 dataset (Hersbach et al. 2020) is greater than $10\,\mathrm{m\,s^{-1}}$.

In this way, Ouyed et al. (2023) was able to retrieve about 10^4 wind vectors at $1° × 1°$ resolutions per pressure level per day, with the root-mean-square vector differences between retrieved AMVs and ERA5 comparable to those for cloud-tracking AMVs (e.g., Santek et al. 2019b), but with much denser vertical coverage (Fig. S2). For instance, horizontal winds were retrieved at all nine pressure levels at 16,143 grids (or 11% of all grids where winds were retrieved at one or more levels) from 1 to 7 July 2020 (or 2,300 wind profiles per day in $1° × 1°$ grids, comparable to radiosonde profiles from about 1,300 upper-air stations worldwide). Compared with collocated radiosonde observations, the 3D AMV errors lie mostly within the geostationary satellite AMV error bounds. The errors increase with altitude or wind speed (which generally increases with altitude), as higher altitudes have much lower water vapor content, making the feature tracking more challenging.

The coarse $(1° × 1°)$ resolution of the water vapor data reduces the number of retrieved wind profiles. More importantly, it increases the magnitude of retrieved (negative) wind speed bias. For instance, using global model moisture field at different resolutions (since such observations are not available), Ouyed et al. (2023) found that increasing the resolution from $1°$ to $0.0625°$ would decrease the speed bias magnitude by a factor of 3. For satellite measurements, this essentially quantifies the resolution requirement (of around $10\,\mathrm{km}$).

The $1°$ resolution of these 3D AMVs is comparable to the horizontal resolution ($90\,\mathrm{km}$) of *Aeolus* wind lidar data for the Rayleigh channel from clear-sky molecule scattering (available for most altitudes), but it is much coarser than the processed horizontal resolution of $10–20\,\mathrm{km}$ used for the Mie channel from particle scattering. As the Mie channel winds are primarily from optically thick cloud tops, from within optically thin clouds, and to a lesser extent from aerosols, they are less frequently available than the Rayleigh channel winds (Martin et al. 2021; Rennie et al. 2021).

If AMVs and lidar winds are collocated over some areas, the lidar winds (that are expected to be more accurate) could be employed to do the bias correction of the AMVs. Using global model simulation data, Ouyed et al. (2021) demonstrated the feasibility of bias correction using machine learning. Specifically, a random forest algorithm is used to extract dynamical information from a small number of collocated, more accurate, measurements (e.g., from wind lidar), mimicked by using "ground truth" plus error structures as a function of reanalysis differences. This bias correction, applied during a second stage of the 3D wind retrieval, substantially reduced the AMV errors from the first stage retrieval that was based on time-differenced water vapor data alone (Fig. S3). Furthermore, this two-stage retrieval has smaller errors than those due to reanalysis differences and collocation errors. It is also advantageous in error-prone regions such as low moisture gradients or velocity fields perpendicular to water vapor gradients. These results confirm the scientific feasibility of the Vientos concept to combine active and passive observations, as part of the global observing system.

Note that a common approach for obtaining 3D winds is to combine passive sounding (of water vapor) with wind lidar measurements and all other available observations (e.g., radiosondes) via four-dimensional data assimilation (e.g., in ERA5). However, observation and model biases need to be actively managed in data assimilation. Future studies should address the optimal way to retrieve 3D winds (e.g., using the above two-stage algorithm plus the use of additional data, such as those from radiosondes and wind lidar, for bias correction) and the optimal way to assimilate wind information in numerical weather prediction (NWP) (e.g., based on the assimilation of radiances, 3D winds, or combination of both). Since data assimilation methods assume knowledge of observational error statistics, any improved

characterization of AMV observation errors also has the potential to improve data assimilation (and hence NWP skill).

Scientific questions and applications using the Vientos measurements

Besides 3D winds, the sounding measurements provide 3D water vapor and temperature data, while the wind lidar provides aerosol measurements (of its optical properties) of the near-storm environment, as summarized in Fig. 1. These simultaneous measurements of 3D winds, temperature, and humidity as well as the aerosol measurements along the satellite track are expected to have substantial impacts on a variety of scientific questions and applications. The immediate effect would be on NWP (e.g., on atmospheric rivers, hurricanes). For instance, Rennie et al. (2021) demonstrated the positive impact of *Aeolus* wind retrievals on global weather forecasts at the ECMWF. Through NWP or directly, these simultaneous measurements can be used for a variety of applications, such as local prediction of convection location/timing, flight route planning in aviation, forecast-informed reservoir operations for water resources and flood control, wind energy prediction and management, transport of pollutants and aerosols, and climate model evaluations. Furthermore, for carbon monitoring, satellite CO_2 and wind measurements plus ocean and land surface flux measurements and emission inventory from individual countries or regions are needed to better constrain global and regional carbon monitoring for international negotiation and policy making.

These measurements can also be used to address science questions, such as the interaction of organized convection [e.g., mesoscale convective systems (MCSs) and hurricanes] with its environment. For instance, MCSs are a cluster of thunderstorms that become organized and form a complex larger than each individual thunderstorm and typically last longer than 6 h. Understanding these systems, their genesis and evolution is very important as they produce 50%–90% of the annual rainfall throughout the tropics (Schumacher and Rasmussen 2020; Roca and Fiolleau 2020). They can also produce hazardous weather such as damaging winds and hail, tornadoes, and flash floods. MCSs are the "building blocks" of the large-scale circulation but are poorly represented in large-scale models (e.g., with a grid size of 0.25° or 1°), and quantifying environment–MCS interactions is fundamental to answer where and when convection initiates and evolves, and how the large-scale circulation changes with global warming.

In a recent study by Galarneau et al. (2023), ERA5 and an automated MCS tracking algorithm were used to investigate the environment preceding MCSs in the tropics. Although it is known that MCSs occur in relatively moist environments, it is unclear how far in advance favorable ingredients (lift, instability, and moisture) in the mesoscale environment precede MCS formation. Using horizontal wind information at 925 and 200 hPa, it was found that
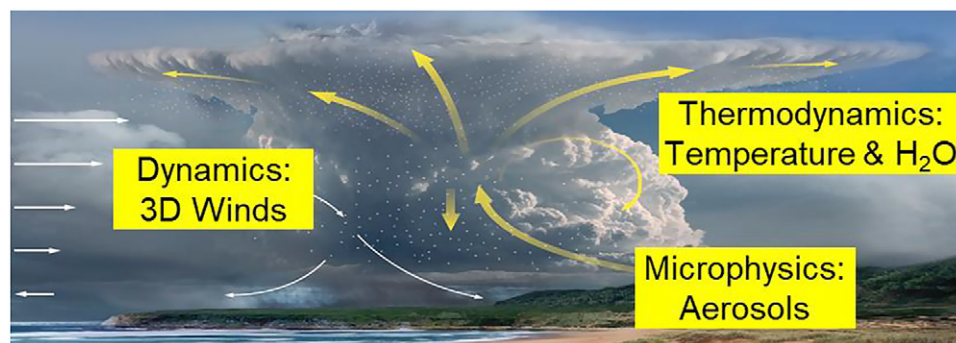

Fig. 1. Vientos summary of simultaneous data of winds, temperature, humidity, and aerosols by combining satellite passive sounders with wind lidar measurements.

mesoscale ascent, inferred from the vertical difference of divergence, preceded all MCSs up to 24 h in advance (Fig. S4c). Similarly, deep saturated conditions preceded all MCSs up to 24 h in advance (Fig. S4a), while lower instability preceded oceanic MCSs (Fig. S4b). Higher instability preceded land MCSs in conjunction with higher temperatures in the boundary layer compared to oceanic MCSs. In all, these results showed that lift, instability, and moisture are altogether important for MCS formation in the tropics and are detectable up to 24 h in advance. Furthermore, significant regional differences were apparent in the vertical structure of wind, temperature, and humidity of preconditioning environments. The statistics of simultaneous measurements of 3D temperature, water vapor, and wind vectors over the full life cycle of MCSs from future satellite missions (e.g., snapshots of MCSs from Vientos) would enable us to observationally study the MCS–environment interactions and enable constraints on reanalysis and modeling-based studies of this issue.

Vientos winds would also provide critical data within and around atmospheric rivers (ARs), enabling full adaptation of resilient management strategies like forecast-informed reservoir operations (Delaney et al. 2020). ARs, which are long, narrow corridors of intense water vapor transport, provide a large majority of water supply on the west coast of continents, but also cause significant damage when they are associated with floods and high winds, and thus are extremely important to forecast correctly on the west coast of the United Stated and globally (Ralph et al. 2019). ARs are associated with documented monitoring gaps of wind and moisture in the global observing system, due to their frequent co-occurrence with clouds and precipitation, and their placement in the lowest 3 km of the atmosphere. On the west coast of the United States, the AR Reconnaissance program functions to fill this gap in observations (Ralph et al. 2020), and Vientos would complement this effort by observing areas in and near ARs that may be out of the range of the aircraft. New targeting strategies could be developed within AR Reconnaissance that leverage the functionality of Vientos. Additionally, Vientos would be critical in other regions (e.g., South America, Europe, Australia) that do not currently have the benefit of airborne reconnaissance, and the programs could be carefully designed to complement each other. We are currently retrieving AMVs in 0.25° grids as a follow-up of Ouyed et al. (2023) and will then quantify their impacts on AR prediction and their synergy with AR Reconnaissance airborne measurements.

Architecture of Vientos and the pathway forward

Passive sounders for water vapor and temperature measurements could be microwave (MW) and/or hyperspectral infrared (IR) radiometers. IR sounders would have a higher horizontal resolution (e.g., 3–10 km) and higher vertical resolution (e.g., ~1.5–2 km) than MW sounders (e.g., 10–30 km for horizontal resolutions and ~2–3 km for vertical). While IR sounding is available for clear-sky or partially cloudy-sky conditions, MW sounding is available for all sky conditions (except under heavy precipitation conditions). Depending on the horizontal resolution, a swath width with ~100 pixels is desired for the wind retrievals. It is preferable to combine MW with hyperspectral IR sounders for the temperature and water vapor retrievals (e.g., as used in Ouyed et al. 2023). If budgets are constrained, and only one type of sounder is possible, then MW sounders would be preferable due to the more frequent availability of measurements (under all weather conditions), as the gaps in the retrieved water vapor field (due to clouds obscuring the infrared measurements) would negatively affect the AMV retrievals. To retrieve AMVs, two sounders should be flown in formation to track features of water vapor. While previous studies have indicated that AMVs can be tracked using images that are separated in time by up to 60 min, such a lengthy time interval introduces the possibility that processes other than horizontal advection will have a significant influence on the differences between water vapor

images. Previous feature-matching AMV techniques required a minimum separation time between images to allow for the detection of translation from one pixel to another (e.g., Posselt et al. 2019), but our recent optical flow results indicate robust performance for time separations between 2 and 10 min (Yanovsky et al. 2023). The use of three sounders (if allowed by the budget) would further decrease the retrieval errors and also provide better quality assessment of the retrieved AMVs. The vertical resolution of AMVs can also be increased by lidar measurements of finely resolved wind profiles over clear-sky conditions, and we are currently addressing this issue using machine learning.

One example of the MW sounder is the Vientos Sounder Radiometer (VISR) in a 12U volume, built by Jet Propulsion Laboratory (JPL). VISR has four subsystems: antenna, radio frequency front end, command and data handling electronics, and the scan mechanism. It has its heritage from several prior satellite missions (including TEMPEST-D; Padmanabhan et al. 2021). It uses four channels around 118 GHz and four channels near 183 GHz to retrieve the temperature and water vapor profiles with a vertical resolution of 2–3 km and horizontal resolution of ~20 km. All subsystems of VISR are at technology readiness level (TRL) 9 and the VISR as a whole is at TRL 6.

The MW sounder's capability can be significantly improved by incorporating additional frequencies near 240, 310, 380, 664, and 850 GHz (Jiang et al. 2019). This instrument expands the system's functionality with its 15 channels, enabling it to achieve a vertical resolution of approximately 2 km when retrieving the cloud ice, temperature, and water vapor profiles. Moreover, it accurately determines cloud ice properties such as effective radius and ice water content. By employing a larger antenna and transitioning to a larger spacecraft (class C), the horizontal resolution of CubeSats (class-D spacecraft) can be improved from approximately 20 km to around 10 km in a SmallSat.

One example of the IR sounder is the CubeSat Infrared Atmospheric Sounder (CIRAS; Pagano et al. 2022), built by JPL. CIRAS is a space-based infrared sounder concept designed to measure temperature and water vapor profiles in a CubeSat compatible volume. CIRAS has its heritage from AIRS (aboard NASA's *Aqua* satellite) that has been operational since 2002, but CIRAS's power, mass, and size are just 9.0%, 2.3%, and 0.45% of those from AIRS. CIRAS uses 625 spectral channels from 4.08 to 5.13 μm at 13.5 km horizontal resolution and 1,500 km swath from 600 km orbit, along with a zoom mode for 3.5 km horizontal resolution and 245 km swath. Figure 2 illustrates the CIRAS flight concept. At present, CIRAS is at TRL 5 and is progressing toward TRL 6.

For the wind lidar, ESA's *Aeolus* has successfully demonstrated the first spaceborne Doppler wind lidar mission technology and its positive impact for NWP and scientific studies using both wind and aerosol/particle products. Its laser system generates a series of short light pulses in the ultraviolet spectrum at 355 nm. ESA member states approved the design of the follow-on mission (Aeolus-2) in late 2022 incorporating the lessons learned from *Aeolus* with improved random and systematic wind errors, horizontal and vertical resolution, and improved capabilities for aerosol sensing (Heliere et al. 2021). For instance, Aeolus-2 is designed with a 1.5 m telescope with improvements in mechanical–thermal design and control based on the experience with *Aeolus* and dedicated thermal tests performed in orbit with the *Aeolus* telescope. It is also designed with increased laser energy and lidar optical efficiency compared to *Aeolus*—both to accommodate a higher altitude orbit of 400 km for a longer lifetime and a better random error of 2 to 2.5 m s^{-1} for the horizontal line-of-sight (LOS) wind component in clear air and better than 2 m s^{-1} for aerosol/cloud LOS winds. The member states of ESA's partner, the European Organisation for the Exploitation of Meteorological Satellites (EUMETSAT), also approved the early stage work of Aeolus-2 in late 2022, with the final approval expected in 2025 for a series of two satellites flying in the time frame from 2030 to 2040.
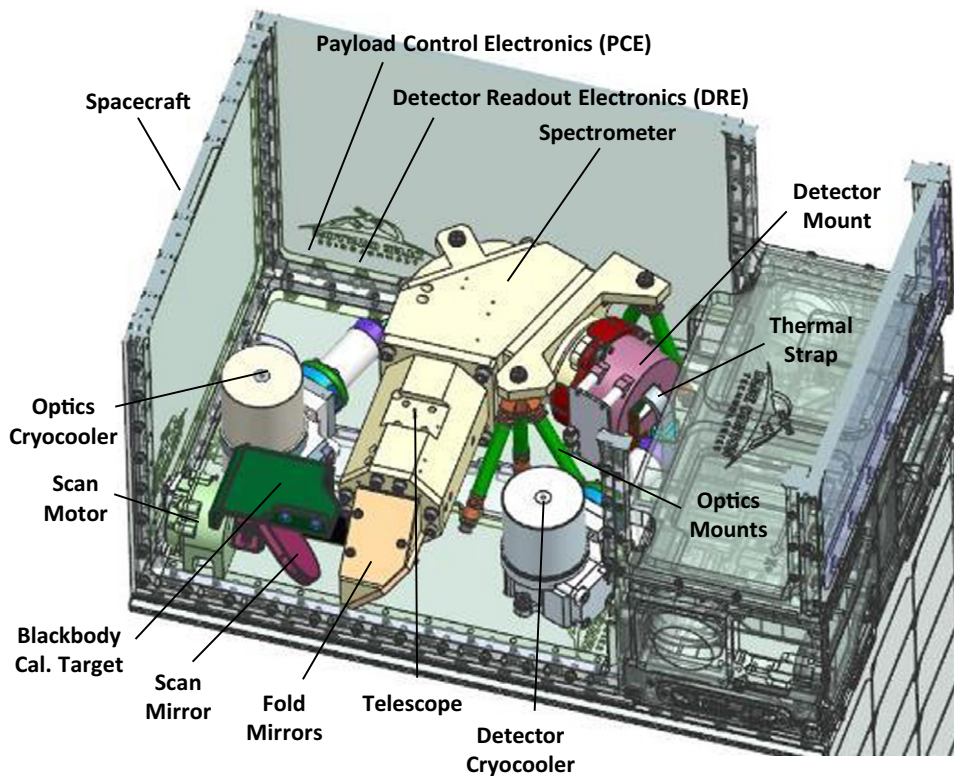
Fig. 2. The CIRAS flight concept occupying a 4U volume, shown in a 12U CubeSat.

For a U.S.-based Doppler wind lidar, building on the heritages of *CALIPSO*, *ICESat-2*, and *Aeolus* satellite lidars, Ball Aerospace built the autonomous Optical Autocovariance Wind Lidar (OAWL; with the system presented in Fig. 3 of Tucker et al. 2018) and demonstrated its performance from high-altitude aircraft. Single and dual LOS OAWL systems (Tucker et al. 2018) have been demonstrated at both the green (532 nm) and ultraviolet (355 nm) laser system wavelengths. A proposed space-based design concept for aerosol and molecular winds would provide LOS winds from the surface up to ~25 km altitude, with 10–100 km along-track resolution and 0.25–1 km vertical resolution. For a system with similar laser and telescope parameters as *Aeolus*, Mie (aerosol) wind precision is expected to be ~1–3 m s⁻¹ in areas where aerosol loading is sufficient, while molecular (Rayleigh) winds would vary from 2 to 8 m s⁻¹ with increasing altitude. Differences relative to *Aeolus* are due to taking the fully transmissive quadrature Mach–Zehnder interferometer approach (versus the filter approach used on *Aeolus*, which exhibits lower signal efficiency). While most OAWL components are at TRL 6 or higher, the U.S.-developed laser and interferometer are at TRL 5, though OAWL could use the same laser used on *Aeolus*. Advancement to TRL 6 requires thermal vacuum chamber testing in final design configuration, requiring standard engineering efforts, without technical challenges. OSSEs have demonstrated very significant potential for OAWL to improve atmospheric analyses and NWP (Atlas et al. 2015).

It would be optimal to obtain lidar 3D winds (using multiple lidars with dual LOS winds), but that is too costly. Dual LOS winds are possible and would provide vector shear for a curtain, relevant for many processes, but they are more expensive than single LOS winds. Curtains of single vector components can be used for process studies too, in particular in combination with 3D winds from passive sounders. Adding a single LOS OAWL system, in an offset orbit relative to *Aeolus*, would provide the global NWP with 2 times the information (Marseille et al. 2008). Efforts are under way regarding the optimal way of using single LOS winds to bias correct the AMVs (e.g., bias correcting one wind component, bias correcting both wind

components by assuming a relationship between the biases in the two components or by using some conservation, such as vorticity, to transfer the bias correction from one component to another).

Based on various trade analyses of costs, risks, and science returns, one option for the Vientos architecture is to use two or more SmallSats (with propulsion) separated by ~10 min, each hosting MW and IR sounders, to form a train with the wind lidar (OAWL or Aeolus-2) in between. The combination of MW and IR sounders will have two benefits: increased horizontal and vertical resolutions of the data (from IR sounders); and increased coverage (yield) of the retrieved winds (from MW sounders in cloudy regions). The formation of a train with Aeolus-2 is particularly attractive, as Aeolus-2 has a high probability of flight in the 2030s. The merged level 3 products of temperature, humidity, and wind profiles are expected to be at around 10 km (horizontal) and 1.5 km (vertical) resolutions. Besides the costs of Aeolus-2 (to be covered by ESA and EUMETSAT), the remaining costs primarily depend on the requirement for class-C or class-D missions and the number of SmallSats. Note that the separation time of ~10 min is determined by the dual requirement of large-enough overlapped swath (or short-enough separate time) between two satellites for AMV retrievals and long enough separation time to reliably retrieve AMVs considering uncertainties in the retrieved water vapor fields.

A second option for Vientos architecture is to use a single spacecraft containing two sounders and the wind lidar in a dawn–dusk sun-synchronous orbit at 450–500 km altitude. The two microwave sounder radiometers are pointed in the ram and wake directions at 50°, providing >2 min of separation time between their respective measurements. Our recent study (Yanovsky et al. 2023) demonstrated that this separation time is sufficient to retrieve 3D AMVs using the optical flow algorithm (while it is too short for the traditional feature-matching method). A wind lidar (e.g., OAWL) is pointed 35° off nadir, cross track in the starboard direction, facing the dusk side of the orbit, just as *Aeolus* has demonstrated. The merged level 3 products of temperature, humidity, and wind profiles are expected to be at about 30 km (horizontal) and 2 km (vertical) resolutions. More careful trade-off analysis is needed to determine the altitude: a lower altitude is preferable for the lidar measurements, while a higher altitude is preferable for a larger separation time for AMV retrieval, possibly without the use of propulsion. The mission cost is dominated by the cost of lidar and large spacecraft.

While Vientos emphasizes the synergy between passive sounders and wind lidar, the use of passive sounders alone for 3D AMV retrievals (along with 3D water vapor and temperature measurements) remains valuable (e.g., Maschhoff et al. 2019).

With these options, Vientos will also provide synergy with the vertical wind measurements, e.g., via the NASA Atmosphere Observing System mission (https://aos.gsfc.nasa.gov/) or microwave high-resolution sounders (Brogniez et al. 2022).

Moving forward, the Vientos concept developments require: further architecture trade analyses through OSSEs, engineering evaluations, and cost estimates; quantification of the synergistic values of combining passive sounders and wind lidar using instrument simulators and OSSEs (which depends on the specific instrument performance and architecture); further studies on the wind retrievals (as part of 4D data assimilation versus wind retrievals using satellite measurements plus auxiliary data); and multiagency and/or international collaborations to cover the costs of the whole mission, including the calibration/validation field campaigns after the launch. The cost caps like those for the class-C NASA Earth System Explorer mission competition afford wind retrievals derived from passive-only microwave and IR soundings and possibly the first option above (with Aeolus-2). With additional funding attained by joining resources from multiple organizations, the first two options (with OAWL) above become possible. Finally, we emphasize that, while Vientos is based on our efforts,

the concept can be applied by any other countries/organizations, and we would be equally happy if it is implemented by others.

Data availability statement. This study does not generate any new data.

References

Alexander, L. V., M. Bador, R. Roca, S. Contractor, M. G. Donat, and P. L. Nguyen, 2020: Intercomparison of annual precipitation indices and extremes over global land areas from in situ, space-based and reanalysis products. *Environ. Res. Lett.*, **15**, 055002, https://doi.org/10.1088/1748-9326/ab79e2.

Apke, J. M., Y.-J. Noh, and K. Bedka, 2022: Comparison of optical flow derivation techniques for retrieving tropospheric winds from satellite image sequences. *J. Atmos. Oceanic Technol.*, **39**, 2005–2021, https://doi.org/10.1175/JTECH-D-22-0057.1.

Atlas, R., and Coauthors, 2015: Observing system simulation experiments (OSSEs) to evaluate the potential impact of an Optical Autocovariance Wind Lidar (OAWL) on numerical weather prediction. *J. Atmos. Oceanic Technol.*, **32**, 1593–1613, https://doi.org/10.1175/JTECH-D-15-0038.1.

Baker, W. E., and Coauthors, 2014: Lidar-measured wind profiles: The missing link in the global observing system. *Bull. Amer. Meteor. Soc.*, **95**, 543–564, https://doi.org/10.1175/BAMS-D-12-00164.1.

Belmonte-Rivas, M., and A. Stoffelen, 2019: Characterizing ERA-Interim and ERA5 surface wind biases using ASCAT. *Ocean Sci.*, **15**, 831–852, https://doi.org/10.5194/os-15-831-2019.

Brogniez, H., and Coauthors, 2022: Time-delayed tandem microwave observations of tropical deep convection: Overview of the C²OMODO mission. *Front. Remote Sens.*, **3**, 854735, https://doi.org/10.3389/frsen.2022.854735.

Delaney, C. J., and Coauthors, 2020: Forecast informed reservoir operations using ensemble streamflow predictions for a multi-purpose reservoir in Northern California. *Water Resour. Res.*, **56**, e2019WR026604, https://doi.org/10.1029/2019WR026604.

Folger, K., and M. Weissmann, 2016: Lidar-based height correction for the assimilation of atmospheric motion vectors. *J. Appl. Meteor. Climatol.*, **55**, 2211–2227, https://doi.org/10.1175/JAMC-D-15-0260.1.

Galarneau, T. J., X. Zeng, R. D. Dixon, A. Ouyed, H. Su, and W. Cui, 2023: Tropical mesoscale convective system formation environments. *Atmos. Sci. Lett.*, **24**, e1152, https://doi.org/10.1002/asl.1152.

Hautecoeur, O., R. Borde, and P. Heas, 2020: 3D wind fields extracted from EUMETSAT IASI level 2 products. EUMETSAT Doc., 19 pp., www-cdn.eumetsat.int/files/2020-04/pdf_amv_meet_17_iasi_3d_winds.pdf.

Heliere, A., D. Wernham, G. Mason, and A. G. Straume, 2021: Aeolus-2 mission pre-development status. *Proc. SPIE*, **11858**, 118580C, https://doi.org/10.1117/12.2599797.

Hersbach, H., and Coauthors, 2020: The ERA5 global reanalysis. *Quart. J. Roy. Meteor. Soc.*, **146**, 1999–2049, https://doi.org/10.1002/qj.3803.

Jiang, J. H., and Coauthors, 2019: Simulation of remote sensing of clouds and humidity from space using a combined platform of radar and multifrequency microwave radiometers. *Earth Space Sci.*, **6**, 1234–1243, https://doi.org/10.1029/2019EA000580.

Marseille, G. J., A. Stoffelen, and J. Barkmeijer, 2008: Impact assessment of prospective space-borne Doppler wind lidar observation scenarios. *Tellus*, **60A**, 234–248, https://doi.org/10.1111/j.1600-0870.2007.00289.x.

Martin, A., M. Weissmann, O. Reitebuch, M. Rennie, A. Geiß, and A. Cress, 2021: Validation of Aeolus winds using radiosonde observations and numerical weather prediction model equivalents. *Atmos. Meas. Tech.*, **14**, 2167–2183, https://doi.org/10.5194/amt-14-2167-2021.

Maschhoff, K., J. Polizotti, H. Aumann, J. Susskind, D. Bowler, C. Gittins, M. Janelle, and S. Fingerman, 2019: Concept development and risk reduction for MISTiC winds, a micro-satellite constellation approach for vertically resolved wind and IR sounding observations in the troposphere. *Remote Sens.*, **11**, 2169, https://doi.org/10.3390/rs11182169.

McCarty, W., D. Carvalho, I. Moradi, and N. C. Privé, 2021: Observing system simulation experiments investigating atmospheric motion vectors and radiances from a constellation of 4–5-μm infrared sounders. *J. Atmos. Oceanic Technol.*, **38**, 331–347, https://doi.org/10.1175/JTECH-D-20-0109.1.

National Academies of Sciences, Engineering, and Medicine, 2018: *Thriving on Our Changing Planet: A Decadal Strategy for Earth Observation from Space.* National Academies Press, 716 pp., https://doi.org/10.17226/24938.

Ouyed, A., X. Zeng, L. Wu, D. Posselt, and H. Su, 2021: Two-stage artificial intelligence algorithm for calculating moisture-tracking atmospheric motion vectors. *J. Appl. Meteor. Climatol.*, **60**, 1671–1684, https://doi.org/10.1175/JAMC-D-21-0070.1.

——, N. Smith, X. Zeng, T. Galarneau, H. Su, and R. D. Dixon, 2023: Global three-dimensional water vapor feature-tracking horizontal wind using hyperspectral infrared sounder data from overlapped tracks of two satellites. *Geophys. Res. Lett.*, **50**, e2022GL101830, https://doi.org/10.1029/2022GL101830.

Padmanabhan, S., and Coauthors, 2021: TEMPEST-D radiometer: Instrument description and prelaunch calibration. *IEEE Trans. Geosci. Remote Sens.*, **59**, 10213–10226, https://doi.org/10.1109/TGRS.2020.3041455.

Pagano, T. S., D. Johnson, J. McGuire, M. Schwochert, and D. Z. Ting, 2022: Technology maturation efforts for the next generation of grating spectrometer hyperspectral infrared sounders. *IEEE J. Sel. Top. Appl. Earth Obs. Remote Sens.*, **15**, 2929–2943, https://doi.org/10.1109/JSTARS.2022.3165168.

Posselt, D. J., and Coauthors, 2019: Quantitative assessment of state-dependent atmospheric motion vector uncertainties. *J. Appl. Meteor. Climatol.*, **58**, 2479–2495, https://doi.org/10.1175/JAMC-D-19-0166.1.

Ralph, F. M., J. J. Rutz, J. M. Cordeira, M. Dettinger, M. Anderson, D. Reynolds, L. J. Schick, and C. Smallcomb, 2019: A scale to characterize the strength and impacts of atmospheric rivers. *Bull. Amer. Meteor. Soc.*, **100**, 269–289, https://doi.org/10.1175/BAMS-D-18-0023.1.

——, and Coauthors, 2020: West Coast forecast challenges and development of atmospheric river reconnaissance. *Bull. Amer. Meteor. Soc.*, **101**, E1357–E1377, https://doi.org/10.1175/BAMS-D-19-0183.1.

Reitebuch, O., 2012: The space-borne wind lidar mission ADM-Aeolus. *Atmospheric Physics: Background—Methods—Trends*, U. Schumann, Ed., Research Topics in Aerospace, Springer, 815–827.

Rennie, M. P., L. Isaksen, F. Weiler, J. de Kloe, T. Kanitz, and O. Reitebuch, 2021: The impact of Aeolus wind retrievals on ECMWF global weather forecasts. *Quart. J. Roy. Meteor. Soc.*, **147**, 3555–3586, https://doi.org/10.1002/qj.4142.

Roca, R., and T. Fiolleau, 2020: Extreme precipitation in the tropics is closely associated with long-lived convective systems. *Commun. Earth Environ.*, **1**, 18, https://doi.org/10.1038/s43247-020-00015-4.

Santek, D., S. Nebuda, and D. Stettner, 2019a: Demonstration and evaluation of 3D winds generated by tracking features in moisture and ozone fields derived from AIRS sounding retrievals. *Remote Sens.*, **11**, 2597, https://doi.org/10.3390/rs11222597.

——, and Coauthors, 2019b: 2018 atmospheric motion vector (AMV) intercomparison study. *Remote Sens.*, **11**, 2240, https://doi.org/10.3390/rs11192240.

Schumacher, R. S., and K. L. Rasmussen, 2020: The formation, character and changing nature of mesoscale convective systems. *Nat. Rev. Earth Environ.*, **1**, 300–314, https://doi.org/10.1038/s43017-020-0057-7.

Stoffelen, A., R. Kumar, J. Zou, V. Karaev, P. S. Chang, and E. Rodriguez, 2019: Ocean surface vector wind observations. *Remote Sensing of the Asian Seas*, V. Barale and M. Gade, Eds., Springer, 429–447, https://doi.org/10.1007/978-3-319-94067-0_24.

——, and Coauthors, 2020: Wind profile satellite observation requirements and capabilities. *Bull. Amer. Meteor. Soc.*, **101**, E2005–E2021, https://doi.org/10.1175/BAMS-D-18-0202.1.

Tucker, S. C., C. S. Weimer, S. Baidar, and R. M. Hardesty, 2018: The optical autocovariance wind lidar. Part I: OAWL instrument development and demonstration. *J. Atmos. Oceanic Technol.*, **35**, 2079–2097, https://doi.org/10.1175/JTECH-D-18-0024.1.

Wu, L., H. Su, X. Zeng, D. J. Posselt, S. Wong, S. Chen, and A. Stoffelen, 2024: Uncertainty of atmospheric winds in three widely used global reanalysis

datasets. *J. Appl. Meteor. Climatol.*, **63**, 165–180, https://doi.org/10.1175/JAMC-D-22-0198.1.

Yanovsky, I., D. Posselt, L. Wu, S. Hristova-Veleva, H. Nguyen, B. Lambrigtsen, and X. Zeng, 2023: Atmospheric motion vector retrieval using the total variation-based optical flow method. *2023 IEEE Int. Geoscience and Remote Sensing Symp.*, Pasadena, CA, IEEE, 3780–3783, https://doi.org/10.1109/IGARSS52108.2023.10282495.

Zeng, X., S. Ackerman, R. D. Ferraro, T. J. Lee, J. J. Murray, S. Pawson, C. Reynolds, and J. Teixeira, 2016: Challenges and opportunities in NASA weather research. *Bull. Amer. Meteor. Soc.*, **97**, ES137–ES140, https://doi.org/10.1175/BAMS-D-15-00195.1.

——, and Coauthors, 2020: Use of observing system simulation experiments in the United States. *Bull. Amer. Meteor. Soc.*, **101**, E1427–E1438, https://doi.org/10.1175/BAMS-D-19-0155.1.